

Extended X-ray emission in the high redshift quasar GB 1508+ 5714 at $z = 4.3$

W. Yuan^{1?}, A. C. Fabian¹, A. Celotti² and P. G. Jonker¹

¹University of Cambridge, Institute of Astronomy, Madingley Road, Cambridge, CB3 0HA

²SISSA, via Beirut, 2-4, 34014 Trieste, Italy

Accepted ??? Received ??? in original form August 15, 2003

ABSTRACT

We report the discovery of extended X-ray emission around the powerful high-redshift quasar GB 1508+ 5714 at $z = 4.3$, revealed in a long Chandra ACIS observation. The emission feature is 3.4 arcsec away from the quasar core, which corresponds to a projected distance of about 25 kpc. The X-ray spectrum is best fitted with a power law of photon index 1.92 ± 0.35 (90 per cent c.l.). The X-ray flux and luminosity reach $9.2 \times 10^{-15} \text{ erg cm}^{-2} \text{ s}^{-1}$ (0.5–8 keV) and $1.6 \times 10^{45} \text{ erg s}^{-1}$ (2.7–42.4 keV rest frame, $\theta = 0.73$, $\mu_m = 0.27$, $H_0 = 71 \text{ km s}^{-1} \text{ Mpc}^{-1}$), which is about 2 percent of the total X-ray emission of the quasar. We interpret the X-ray emission as inverse Compton scattering of Cosmic Microwave Background photons. The scattering relativistic electron population could either be a quasi-static diffuse cloud fed by the jet, or an outer extension of the jet with a high bulk Lorentz factor. We argue that the lack of an obvious detection of radio emission from the extended component could be a consequence of Compton losses on the electron population, or of a low magnetic field. Extended X-ray emission produced by inverse Compton scattering may be common around high redshift radio galaxies and quasars, demonstrating that significant power is injected into their surrounding by powerful jets.

Key words: galaxies: active – galaxies: jets – galaxies: quasars: individual: GB 1508+ 5714 – radiation mechanisms: non-thermal – X-ray: galaxies

1 INTRODUCTION

High redshift active galactic nuclei (AGN) are powerful tools with which to study the evolution of supermassive black holes (SMBH) and their host galaxies at an early epoch. One important issue concerns the feedback from SMBH to the host galaxy by means of kinetic energy input carried in energetic particle flows in the form of jets. Relativistic jets are inferred to be present in high-redshift radio-loud AGN, particularly in blazar-like objects (i.e. with a jet oriented close to the line of sight), from their extremely high luminosities ($\sim 10^{47} \text{ erg s}^{-1}$) and variability in both the X-ray and radio bands (e.g. Fabian et al. 1997, 1999).

In the X-ray band, thanks to the sub-arcsec spatial resolution of the Chandra X-ray Observatory, direct evidence of resolved X-ray jets and extended emission has been obtained in dozens of radio galaxies and quasars (e.g. Chartas et al. 2000, Schwartz et al. 2000, Worrall et al. 2001, Fabian, Celotti & Johnstone 2003b, Harris et al. 2002, Siemiginowska et al. 2003). Models have been proposed to explain the X-ray emission on such scales involving synchrotron, in-

verse Compton scattering of photons of the synchrotron, Cosmic Microwave Background (CMB) and radiation from the AGN nucleus (e.g. Celotti et al. 2001, Tavecchio et al. 2000, Harris & Kravtsov 2002). Inverse Compton scattering of the CMB is particularly relevant at high redshifts since, as pointed out by Schwartz (2002a), the X-ray surface brightness of jets is roughly constant with redshift as a consequence of the steep $(1+z)^4$ increase in the energy density of the CMB. Another factor to consider at high redshifts (above $z \sim 2$) is that the angular size actually increases with redshift. While there have been efforts to search for X-ray jets at high redshifts e.g. up to $z \sim 6$ (Schwartz 2002b), the highest redshift at which a convincing detection has been obtained so far is $z = 3.8$ for the radio galaxy 4C 41.17 as reported by Scharf et al. (2003) recently.

The quasar GB 1508+ 5714 at $z = 4.301$ (Hook et al. 1995) is one of a dozen quasars at redshifts above 4 with strong radio emission ($F_{5\text{GHz}} > 10 \text{ mJy}$). Variability in the X-ray and radio bands, as well as a high X-ray luminosity of $\sim 10^{47} \text{ erg s}^{-1}$ (Moran & Helfand 1997) suggests relativistically beamed X-ray and radio emission of a blazar type. In several high redshift quasars soft X-ray spectral attening has been found (e.g. Boller et al. 2000, Yuan et al. 2000,

? E-mail: wmy@ast.cam.ac.uk (wy)

arXiv:astro-ph/0309318v1 11 Sep 2003

Fabian et al. 2001). However, in our XMM observation of GB 1508+ 5714 (paper in preparation) no evidence for such an effect was found (see also Moran & Helfand 1997).

We report here on the discovery of extended X-ray emission in GB 1508+ 5714 from a long Chandra ACIS-S observation (Sect. 2) and discuss its possible origin (Sect. 4). We used $H_0 = 71 \text{ km s}^{-1} \text{ Mpc}^{-1}$, $\Omega_m = 0.73$, and $\Omega_b = 0.27$ to calculate luminosities and distances throughout the paper. Errors quoted are at the 1 σ level unless stated otherwise.

2 OBSERVATIONS AND DATA ANALYSIS

The quasar GB 1508+ 5714 was observed with Chandra with its back-illuminated CCD ACIS-S3 in the faint mode for a duration of 91.8 ksec starting from 2001 June 10. The data were taken from the Chandra archive (PI: Paerels, Paerels et al. 2002). The target was placed close to the nominal aim point with a small offset of 20 arcsec. The data analysis was performed using the standard CIAO tools (version 2.3, caldb version 2.21). The good exposure time is 88.97 ksec after filtering the data. A level 2 event file was created from level 1 data following the standard procedure. Events with grade of 0, 2, 3, 4, 6 were selected. Only events with energy in the 0.3–8 keV range were included.

2.1 Extended X-ray emission feature

The X-ray image of GB 1508+ 5714 in the 0.3–2 keV band is shown in Fig. 1, with the bin size as 1 original pixel of the CCD, i.e. 0.5 arcsec. We used the 0.3–2 keV band for spatial analysis as the Chandra point spread function (PSF) is best understood within this energy range. The core of the X-ray source is unresolved (the source profile being consistent with that of the PSF) and coincident with the optical/radio position of the quasar (15h10m 02.9s + 57d02m 43s J2000). In addition, to the south-west of the core the X-ray emission is apparently resolved and extended. This extended part of the emission is peaked at 15h10m 02.6s + 57d02m 42s (indicated by a smaller contour of 22 ctspixel⁻¹ level in Fig. 1), which is 3 arcsec away from the position of the quasar core and has a position angle of 250° relative to the core. At a redshift of 4.3, this angular distance corresponds to a projected distance of 21 kpc. The feature extends up to 4 arcsec (28 kpc) from the core along the direction defined by this position angle, and spans 2 arcsec (14 kpc) in the transverse direction.

The source counts of the extended emission were extracted from a circle with a radius of 2.5 pixel (1.25 arcsec), as shown in Fig. 2. It covers the extended emission region and lies outside the circle of 95 per cent encircled energy of the central point source with a radius of 1.4 arcsec (the circle around the core in Fig. 2). To extract background counts, we have to take into account the contamination of photons from the nearby core. We define three circles as background regions which have the same sizes and are located at the same radial distances from the quasar core as the source region (see Fig. 2). Since the PSF of the point source is nearly symmetric (the object is almost on-axis), the contamination from the quasar core is expected to be eliminated to a large extent with this background subtraction. In the 0.3–8 keV

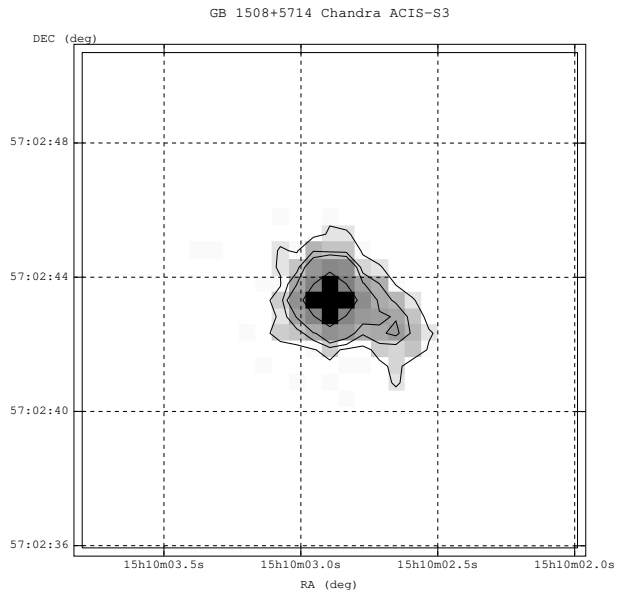


Figure 1. X-ray image of the quasar GB 1508+ 5714 in the 0.3–2 keV band on 15 \times 15 arcsec scales. The bin size is 0.5 arcsec, i.e. the original CCD pixel is used (logarithmic grey scale, cut-off range 2–200 ctspixel⁻¹). The X-ray emission is extended in the south-west direction up to 4 arcsec (a projected distance of 28 kpc). The contours are at levels of 2.5, 10, 22, 180 ctspixel⁻¹.

band, the total number of counts in the extended source region is 158. The averaged number of counts in each of the three background regions is 22.3, consistent with what is expected from the contribution of the core for the Chandra PSF. The net source counts of the extended emission (with possible contamination from the quasar core excluded) is estimated to be 136 \pm 13, yielding a highly significant detection (11 σ). Its count rate is 1.50 \pm 0.14 \times 10⁻³ ctss⁻¹ (0.3–8 keV), which is 2.5 per cent of that of the quasar (0.06 ctss⁻¹).

We do not consider this extended emission feature as an artifact. In the data validation and verification report the observation and data processing were noted as having a good aspect solution and no identified problem. Furthermore, the count rates of the extended emission show no sign of time variability on any timescale during the observation.

We attempted to distinguish whether the extended emission is point-like or diffuse by modelling the 2-D quasar core emission using the Chandra PSF and then subtracting the model from the image data. However, the result is inconclusive, given the small number of net source counts of the extended emission in contrast to the nearby bright quasar core, and the uncertainty in modelling the PSF. Future deep X-ray observations with higher spatial resolution are needed to resolve this emission.

2.2 X-ray spectrum of the extended emission

The spectra of the extended emission and the background were extracted from the regions described above. The RMF and ARF files were created at the source position. We performed spectral fitting using XSPEC (v.11.2). The effect of degradation in the ACIS quantum efficiency was taken into account by applying the apply_acisabs provided in

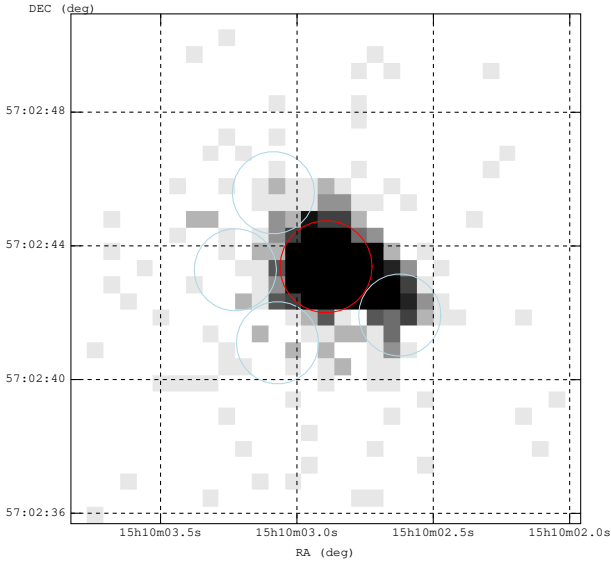


Figure 2. The same image as in Fig 1 with a different grey scale cut-off range ($0\{80\text{ctspixel}^{-1}$). Over-plotted is the circle of 95 per cent encircled energy for the quasar core (central, 1.4 arcsec in radius). Also plotted are the circular regions used for extracting the extended emission (west-most) and the background (eastern three).

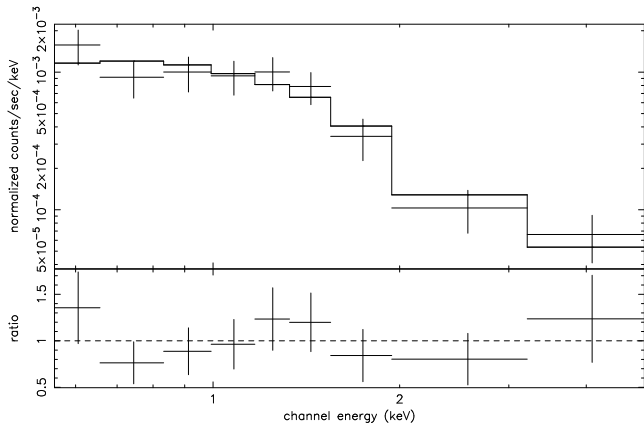


Figure 3. The X-ray spectrum of the extended emission feature and the best-fit absorbed power law model (upper panel). The ratio of the data to the model is also shown (lower panel).

CIAO (Chartas & Getman 2003). Given the small number of source counts, the spectrum was binned to have at least 15 counts per energy bin, and the C-statistic is adopted in the spectral fitting. Absorption with Galactic column density ($1.6 \times 10^{20} \text{ cm}^{-2}$) was included and the value was fixed in the fit. The background-subtracted spectrum is best fitted with a power law model (C-stat= 4.2 for 9 bins), yielding a photon index of $1.92^{+0.38}_{-0.33}$ (90 per cent confidence level). The spectrum and fitted residuals are shown in Fig 3. A redshifted thermal plasma model (Raymond-Smith) gave a slightly worse but acceptable fit (C-stat= 5.2 for 9 bins) with a rest frame temperature $T = 172^{+21.1}_{-7.4} \text{ keV}$.

The unabsorbed flux density in the 0.5-8 keV band is $92 \times 10^{-15} \text{ erg cm}^{-2} \text{ s}^{-1}$, using the best-fit power law

model, which corresponds to a $2.7(42.4 \text{ keV})$ luminosity of $1.6 \times 10^{45} \text{ erg s}^{-1}$ in the quasar rest frame.

3 CONSTRAINTS FROM OTHER WAVEBANDS

In the radio band, the quasar was detected as a radio source at low and high frequencies, e.g. 222 mJy at 365 MHz (Douglas et al. 1996), 279 mJy at 4.85 GHz (Becker et al. 1991). The radio emission GB 1508+ 5714 was unresolved with VLA A-configuration at 1.4 (234 mJy) and 8.4 GHz (152 mJy) with 5-m observations (Moran & Helfand 1997). On mas scales the quasar remains unresolved with VLBI observations (the EVN, Frey et al. 1997). The compactness of the radio emission suggests that the postulated radio jet is closely aligned to the line of sight.

The optical imaging data for GB 1508+ 5714 taken with the Wide-Field-Camera at the Isaac Newton Telescope show no emission at the position of the extended X-ray emission at 5 limiting magnitudes of 23.20 and 23.57 in the i^0 and g^0 -band, respectively. These data also suggest that it is unlikely that the extended X-ray emission is coming from a foreground or background AGN. This is because at this X-ray flux level the majority of AGNs have I-band magnitudes brighter than $I < 23.3$ (corresponds to $f_x/f_{opt} > 610$), as found in the Chandra deep surveys (e.g. Alexander et al. 2001). In the following section of this paper we consider only the most likely scenario that the extended X-ray emission is associated with the quasar.

4 THE EMISSION MECHANISM AND NATURE OF THE EXTENDED EMISSION

We have found a blob of extended X-ray emission about 3 arcsec away from the powerful blazar GB 1508+ 5714. This corresponds to a projected distance of about 21 kpc, but could be 100 kpc or more if it is the outer part of the blazar jet. Interpretation of this X-ray emission is not straightforward given the paucity of information from other wavebands.

The most obvious emission mechanism is inverse Compton scattering of Cosmic Microwave Background photons. At the quasar redshift of 4.3 the energy density in the CMB is 790 times that now. The relativistic electron population scattering the CMB photons is plausibly due to the blazar jet. It can either be a quasi-static diffuse cloud fed by the jet, or an outer extension of the jet with a bulk Lorentz factor ~ 10 . This last possibility has been proposed for the X-ray jets seen around several lower redshift quasars (e.g. Celotti et al. 2001, Tavecchio et al. 2000, Siemiginowska et al. 2003).

Infrared emission from the blazar itself may contribute to the seed photons for inverse Compton scattering (e.g. Brunetti et al. 1997) but the emission would have to be very luminous ($\sim 10^{48} \text{ erg s}^{-1}$) to compete with the CMB at that redshift. We have found no published far infrared measurements of this object with which to make an estimate of any such contribution.

An important issue is to explain why the X-ray blob is

not seen at radio wavelengths. High resolution radio imaging by the EVN (Frey et al. 1997) shows that the source is unresolved on the 10 milliarcsec scale at 5 GHz. The flux in that component is within 2 mJy of the total flux seen with the VLA. Although the source may vary between the observations, we shall assume that the radio emission from this component is less than a few mJy.

The lack of a detection of the extended component could be a consequence of Compton losses on the electron population, or of a low magnetic field. If the electrons have no relativistic bulk motion, then the X-ray emission requires electrons with Lorentz factor $\gamma \approx 10^3$ with $\beta \approx 1$. The magnetic field in the same region required to produce 5 GHz radio emission in our rest frame is $B \approx 10^{-2} \gamma^2$ G. The energy density of this magnetic field is about 10^4 times that in the CMB, which would be reflected in the radio luminosity being 10^4 times that in the X-ray, rather than the observed limit of 0.1. Consequently the magnetic field must be much lower and much higher in order to produce 5 GHz radio emission.

The lifetime of the electrons provides a strong constraint, $t_c \approx 3.2 \times 10^6 \gamma^{-1}$ yr. Radio-emitting electrons with $\gamma \approx 10^5$, and a plausible galactic field of 1 G, thus have a lifetime of only 3×10^4 yr. If these particles diffuse out (without further acceleration) at a velocity $v \approx 0.1c$ then they will have gone only 1 kpc while emitting in the radio. X-ray emitting electrons with $\gamma \approx 10^3$ can have travelled 100 times further. So the lack of any corresponding strong radio emission from the X-ray blob could just be due to Compton losses on the highest energy electrons required to make that radio emission.

We note that the optical limits may require that the electron population has a low energy tumo at < 100 .

If the X-ray emission is produced instead within a relativistic jet with $\beta \approx 10$, the required γ from the X-rays drops by 10 and the lifetime of the electrons t_c by a similar factor. The magnetic field can now be higher without any conflict with the radio limit. Deep radio and optical imaging will provide valuable information with which to discriminate between the possibilities.

It is thus likely that the luminous X-ray blob is a by-product of the powerful inner blazar jet which must have been in operation for at least 10^5 yr (the light crossing time to the blob). It only represents about one per cent of the power of the blazar but is emitted at considerable distance from the nucleus. There should be energetic protons and nuclei associated with the electrons which mean that significant energy is being deposited into the halo of the host galaxy. The fact that it is best seen in the X-ray band is a consequence of the steep $(1+z)^4$ increase in the energy density of the CMB target photons for inverse Compton scattering. The predominance of extended inverse Compton X-ray emission in distant radio sources is becoming apparent from the results on 3C 294 at $z=1.786$ (Fabian et al. 2003a), 3C 9 (Fabian, Celotti & Johnstone 2003b) and 4C 41.17 (Scharf et al. 2003). Further high resolution X-ray observations of distant radio sources should give more insight into this energy channel, which could influence the formation and growth of galaxies, groups and clusters.

ACKNOWLEDGEMENTS

ACF thanks the Royal Society for their support. ACF acknowledges the MUR (COFIN) and ASI for financial support. The Chandra data presented in this paper were obtained from the CXC Chandra archive. We thank all the members of the Chandra team for making the observation and data analysis available. This work has made use of the INT-WFC optical imaging data obtained by the XID imaging programme of the XMM Survey Science Centre (XMM SSC). This research has made use of the NASA/IPAC Extragalactic Database (NED).

REFERENCES

- Alexander D M., Brandt W N., Homschmeier A E., et al. 2001, *AJ*, 122, 2156
- Becker R H., White R L., Edwards A L., 1991, *ApJS*, 75, 1
- Boller, T h., Fabian, A C., Brandt, W N., Freyberg, M J., 2000, *MNRAS*, 315, L23
- Brunetti G., Setti G., Comastri A., 1997, *A&A*, 325, 898
- Celotti A., Ghisellini G. & Chiaberge M., 2001, *MNRAS*, 321, L1
- Chartas G., et al., 2000, *ApJ*, 542, 655
- Chartas G. & Getman K., 2003, Chandra data analysis CIAO web page
- Douglas J N., Bash F N., Bozayan F A., 1996, *AJ*, 111, 1945
- Fabian A C., Brandt W N., McMahon R G., Hook I M., 1997, *MNRAS*, 291, L5
- Fabian A C., Celotti A., Pooley G., et al. 1999, *MNRAS*, 308, L6
- Fabian A C., Celotti A., Iwasawa K. et al., 2001, *MNRAS*, 323, 373
- Fabian A C., Sanders J S., Crawford C S., Ettori S., 2003a, *astro-ph/0301468*
- Fabian A C., Celotti A., Johnstone R M., 2003b, *MNRAS*, 338, L7
- Frey S., Gurvits L.I., Kellermann K.I., Schilizzi R.T., Pauliny-Toth I.I.K., 1997, *A&A*, 325, 511
- Harris D E., Finoguenov A., Bridle A H., et al. 2002, *ApJ*, 580, 110
- Harris D E. & Krawczynski H., 2002, *ApJ*, 565, 244
- Hook I M., McMahon R G., Patnaik A R., et al. 1995, *MNRAS*, 273, L63
- Moran E C. & Helfand D J. 1997, *ApJ*, 484, L95
- Paerels F., Petric A., Telis G., Helfand, D J., 2002, abstract for American Astronomical Society Meeting 201, No.97.03
- Schwartz D A., et al., 2000, *ApJ*, 540, L69
- Schwartz D A., et al., 2002a, *ApJL*, 569, 23
- Schwartz D A., et al., 2002b, *ApJL*, 571, 71
- Sieriginowska A., Stanghellini C., Brunetti G., et al. 2003, *astro-ph/0306129*
- Scharf C., Smail I., Ivison R., et al., 2003, *astro-ph/0306314*
- Tavecchio F., Maraschi L., Sambruna R M., Urry C M., 2000, *ApJ*, 544, L23
- Worrall D M., Birkinshaw M., Hardcastle M J., 2001, *MNRAS*, 326, L7
- Yuan W., Matsumoto M., Wang, T., et al., 2000, *ApJ*, 545, 625

This paper has been typeset from a $\text{T}_{\text{E}}\text{X}$ / $\text{L}_{\text{A}}\text{T}_{\text{E}}\text{X}$ file prepared by the author.